Radiotherapy Planning of Gliomas

Subjects: Imaging Science & Photographic Technology

Contributor: Francesco Cicone, Antonella Castellano, Michele Bailo

The accuracy of target delineation in radiation treatment (RT) planning of cerebral gliomas is crucial to achieve high tumor control, while minimizing treatment-related toxicity.

Keywords: radiation treatment planning ; glioma ; advanced MRI ; magnetic resonance spectroscopy ; perfusion-weighted imaging ; diffusion-weighted imaging ; hypoxia ; PET ; amino acid radiopharmaceuticals ; FET

1. Introduction

The mainstay of treatment for patients with either low-grade or high-grade gliomas (HGG) is surgical resection followed by a combination of radio and chemotherapy [1][2]. In patients with glioblastoma (GBM), standard treatment consists of maximal surgical resection, radiation treatment (RT) (60 Gy in 2-Gy fractions), and concomitant and adjuvant chemotherapy with temozolomide [3]. In elderly patients, a hypofractionated RT schedule (40 Gy in 15 daily fractions of 2.67-Gy) showed equivalent overall survival (OS), but lower toxicity compared with standard RT [4][5]. Based on the CCTG CE.6/EORTC 26062-22061 phase III trial, hypofractionated RT associated with concomitant and adjuvant temozolomide has become the standard treatment modality for elderly patients with GBM [6]. However, despite aggressive management, approximately 90% of GBM recur locally within two years [1][7]. Postoperative RT at doses of 54–59.4 Gy in 1.8 Gy per fraction is the standard of care for adult grade 2 and 3 gliomas, followed by procarbazine, lomustine, vincristine (PCV chemotherapy), or temozolomide chemotherapy [2].

Modern RT techniques, including intensity-modulated radiotherapy (IMRT), stereotactic RT (SRT), and radiosurgery (SRS), allow better conformality of dose to the target with a subsequent decrease in treatment-related complications [8]. However, late neurocognitive dysfunctions, presenting as diminishing mental capacity for working memory, learning ability, executive function, and attention, remain a major concern for patients with glioma receiving high dose radiation to large brain-volume [9][10].

In this regard, an accurate delineation of tumor volumes and organs at risk (OARs) is critical to ensure maximum target dose and sparing of the surrounding normal brain structures to maintain high tumor control, while minimizing treatment-related toxicity. Most radiation treatment centers are equipped with dedicated computed tomography (CT) scanners that provide precise geometric information of anatomical structures, as well as electron density information for accurate dose calculation in treatment planning systems. Magnetic Resonance Imaging (MRI), using postoperative contrast-enhanced T1-weighted and T2-weighted sequences, has progressively replaced CT imaging because of its excellent soft-tissue contrast, high spatial resolution, and widespread availability. Based on these characteristics, MRI represents the current standard imaging modality for glioma target volume delineation; however, conventional imaging does not provide biological information, such as regional blood volume and microstructural architecture. Limitations of conventional MRI sequences include: (1) Limited capability in differentiating between treatment-related changes and disease progression in previously treated gliomas [11][12][13]; (2) non-specific increase in blood-brain barrier (BBB) permeability in contrast-enhanced T1-weighted sequences, which can reflect BBB disruption rather than truly assessing tumor vascularity; and (3) non-specificity of T2-weighted signal abnormality [14][15][16][17].

To overcome the aforementioned limitations, advanced physiology-based MRI techniques have been developed for biological characterization of brain gliomas, such as MR spectroscopy (MRS), diffusion MRI (dMRI), and perfusion MRI (PWI), providing relevant metabolic, structural, and hemodynamic information for treatment planning and monitoring [18][19][20]. Radionuclide imaging techniques, such as positron emission tomography (PET), are also being increasingly used in the workup of primary brain tumors, as they can provide important diagnostic information regarding the delineation of tumor extent for treatment planning, for the diagnosis of treatment-related changes, and the assessment of treatment response [21][22][23][24].

2. Advanced Physiological MRI for RT Planning of Gliomas: Technical Background and Clinical Results

2.1. MR Spectroscopy (MRS)

Proton MR spectroscopy (^{1}H-MRS) has been largely used to detect and quantify several endogenous cellular metabolites in brain gliomas in vivo, including choline (Cho), N-acetyl-aspartate (NAA), creatine (Cr), lactate (Lac), and lipid (Lip) [25]. As glioma malignancy and grade increase, an abnormal elevation of Cho is observed, due to the elevated membrane phospholipid turnover in actively proliferating tumors, whereas a decrease of the peaks of NAA, a marker of neuronal integrity, and Cr, a marker of bioenergy storage, is detected [26][27][28]. HGG often show the appearance of Lac and Lip peaks, byproducts of anaerobic glycolysis and tissue hypoxia, and cell death and necrosis [28]. As the absolute quantification of MRS-detected metabolites is technically challenging in a clinical setting, semi-quantitative assessment using metabolite ratios is often used. Furthermore, by combining MRS acquisition with spatial localization techniques similar to those used in generating anatomical MR images, a larger volume can be selected to acquire signals from multiple voxels across a 2D slice or 3D cubic volume, to generate semi-quantitative maps of the variations in levels of the different metabolites [29]. This method is known as MR spectroscopic imaging (MRSI), and despite the presence of significant challenges for robust acquisitions of good-quality data, it is the technique of choice for the integration in RT treatment planning. With modern MR systems in a specialized center, the acquisition time for clinically-adapted 3D whole-brain MRSI is on the order of 5–10 min, and the spatial resolution of the voxels obtained is typically 0.5–1 cm^3 [30].

Correlation of in vivo MRSI parameters with ex vivo histologic features from image-guided tissue samples in patients with gliomas showed that areas of elevated Cho and reduced NAA relative to normal brain accurately correlate with regions of increased cellular proliferation, thus indicating a metabolically active part of the tumor [26][31]. The ratio of choline to NAA (Cho/NAA index or CNI), normalized to the contralateral normal tissue, has been used as a semi-quantitative metric to define the extension of the metabolic abnormality in GBM [26][32][33].

Furthermore, in studies comparing differences in the contrast-enhancing (CE) lesion, T2/FLAIR, and metabolic lesions for grade 3 glioma and GBM, the volume of Cho/NAA abnormality is often substantially larger than the contrast-enhancing region and sometimes extends beyond the margins of FLAIR abnormality, thus possibly detecting disease infiltration and predicting areas of newly enhanced lesions after chemoradiation therapy [34][35][36][37][38]. Therefore, in the context of glioma RT planning, MRSI may help improve microscopic disease coverage and prevent marginally recurrent disease [25][39][40][41].

There is interest in targeting MRSI metabolic abnormality by selectively escalating the dose using either IMRT ‘dose painting’ or SRS boosts. Dose painting approaches deliver spatially non-uniform doses with very steep dose gradients, improving normal tissue sparing. By using this method, it is possible to create highly heterogeneous dose distributions within a brain tumor, minimizing the doses to surrounding healthy tissues [42].

Ken et al. simulated the integration of MRSI in the treatment planning system (TPS) for GBM dose painting to prove the dosimetric feasibility of a simultaneous integrated boost (SIB) up to 72 Gy to the volume defined by a Cho/NAA ratio > 2 [43]. In a cohort of 16 GBM patients, they simulated three types of dosimetry plans, one conventional plan of 60-Gy in 3D conformational radiotherapy (3D-CRT), one 60-Gy plan in IMRT, and one 72-Gy plan in SIB-IMRT. Dosimetry plans of 72-Gy SIB-IMRT and 60-Gy IMRT showed a significantly decreased maximum dose to the brainstem (44.00 and 44.30 vs. 57.01 Gy) and decreased high-dose volumes to the normal brain compared to 60-Gy 3D-CRT ($p < 0.05$). This demonstrated that delivering standard doses to conventional targets and higher doses to new target volumes based on the areas of highest Cho/NAA abnormality is possible without increasing the dose to organs at risk [43].

A prospective phase II trial (trial NCT00253448) on 35 GBM patients incorporated a single 15–24 Gy Gamma Knife SRS boost in addition to standard chemoradiation, to be directed at high-risk disease defined by a Cho/NAA ratio >2. Acceptable toxicity and favorable OS compared with historical controls were reported. Specifically, the median survivals for recursive partitioning analysis (RPA) Class 4, 5, and 6 patients were 18.7, 12.5, and 3.9 months, respectively, compared with Radiation Therapy Oncology Group (RTOG) RT-alone historical control survivals of 11.1, 8.9, and 4.6 months. For the 16 of 35 patients who received concurrent TMZ in addition to protocol RT treatment, the median survival was 20.8 months, which compared favorably with the European Organization for Research and Treatment of Cancer (EORTC) historical controls of 14.6 months using RT and TMZ [44].

More recently, a multicenter prospective phase III trial in newly diagnosed GBM (SPECTRO GLIO, trial NCT01507506, estimated study completion date: March 2023) is evaluating the potential survival benefit of a simultaneous integrated boost of IMRT (72Gy/2.4Gy) delivered to the portion of the disease identified by a Cho/NAA > 2 at MRSI [45].

The feasibility of using MRSI to guide dose-escalated RT for newly diagnosed GBM is also under investigation in a single-arm multi-institutional trial using 3D MRSI (trial NCT03137888, estimated study completion in July 2021). The study utilizes the Brain Imaging Collaboration Suite (BrICS), a cloud platform developed by Gurbani et al. that integrates MRSI with standard MRI and enables team members from multiple institutions to work together in RT target delineation. Further outcomes of the study are the 1-year PFS, the OS, and the performance on neurocognitive and quality-of-life (QOL). Data from 18 patients treated using targets created in BrICS have been reported so far without severe toxicities [46].

Further investigation is needed to clarify the potential of MRSI in radiation treatment planning and to standardize the analysis of MRSI spectra [41][46]. In particular, the absence of a common platform across different vendors for 3D MRSI processing and the technical complexity of integrating spectral images in the treatment planning system still represent limitations to the wide implementation of this technique in the RT workflow.

Future directions will also include the possibility to non-invasively detect tumor-specific intracellular metabolites by MRSI, which may also have the potential to assist in treatment planning and monitoring. In particular, intratumoral accumulation of 2-hydroxyglutarate (2HG) resulting from the isocitrate dehydrogenase (IDH) gene mutation in brain gliomas can be quantified in vivo by MRSI [47][48]. 2HG has been recently used as a biomarker to detect the presence and spatial distribution of IDH-mutated cells in gliomas, and the tumor volume identified by 2HG MRSI extends beyond FLAIR pathologic volume in a significant number of patients with IDH-mutant gliomas [49], thus having important implications for radiotherapy planning of this molecular subtype of gliomas. Further studies are warranted to enhance the implementation of this method, still technically challenging, in the clinical setting.

2.2. Diffusion Tensor Imaging (DTI) and MR Tractography

Diffusion tensor imaging (DTI) is a dMRI technique that quantifies the amount and orientation of hindered water diffusion within tissues [50]. As water diffusion is anisotropic in brain white matter, reflecting its organization in bundles of fibers running in parallel, DTI can also be used to map the underlying tissue microstructure [50]. The DTI-derived fractional anisotropy (FA) map reflects fiber directionality and density, as well as the axonal diameter and white matter myelination [51]. DTI has been exploited to depict the spatial orientation of the white matter fiber tracts in the brain by a method called fiber tracking or MR tractography [52]. MR tractography is the only non-invasive method that enables to identify in vivo the main fiber tracts adjacent to or inside brain tumors [53] and is commonly used in glioma preoperative setting to improve neurosurgical planning, guiding the surgical approach to prevent damages to relevant tracts [54]. The rationale for using DTI and MR tractography in RT target delineation is the histopathological evidence that invasive glioma cells migrate preferentially along white matter fiber tracts [55][56]. Furthermore, mathematical models of glioma growth are typically improved by incorporating DTI anisotropy for simulation [57]. Consequently, DTI abnormalities have been largely employed to define the extent of peritumoral microinfiltration beyond the apparent borders on conventional MR imaging [58], supported by histopathological validation from DTI-guided brain biopsies [59]. In addition, the pattern of DTI abnormalities has been shown to predict patterns of tumor recurrence in HGG [60], and the location of progressive tumor spread [61]. As the peritumoral white matter abnormality depicted by DTI can be used to predict the trajectory of invasive tumor cells, then this information could be used to inform RT treatment planning [27][62][63]. This can be particularly relevant for diffusely infiltrating lower-grade gliomas or GBMs featuring large non-contrast-enhancing tumor portions, whose extension might be better characterized by DTI signatures. An anisotropic expansion that considers DTI abnormality may maximize the chances of treating migrating cancer cells, while minimizing the amount of brain tissue exposed to high doses of ionizing radiation [27]. It is worth noting that, in the setting of RT planning, target volumes defined by DTI-derived mathematical glioma growth models showed scarce overlap with the standard CTV, possibly related to the different information conveyed by this technique [64].

Jena et al. retrospectively compared standard planning techniques with individualized plans based on DTI in seven patients with biopsy-proven HGG by performing a dosimetry study to prove that DTI could be used as the basis of a dose escalation strategy [63]. The volume of DTI-based abnormality was added to the conventional GTV to encompass areas at high risk of tumor involvement, and then patient-based, individualized CTVs (CTVI) were generated by adding a 1 cm margin to the DTI+GTV volume. In all cases, DTI was shown to reduce PTV size (mean 35%, range 18–46%), resulting in escalated doses (mean 67 Gy, range 64–74 Gy), with normal tissue complication probability (NTCP) levels that matched the conventional treatment plans. The authors concluded that DTI could individualize RT target volumes by excluding areas of the unaffected brain from the target volume, with consequent CTV reduction. The use of a non-uniform margin from GTV to CTV would allow significant dose escalation, while restricting the risk of normal tissue damage to acceptable levels [63].

Berberat et al. evaluated the feasibility of using DTI for RT target volume delineation in 13 GBM patients [62]. A DTI-CTV was generated by adding the DTI abnormality to the contrast-enhancing lesion, and this volume was isotropically expanded by 1 cm and then extended for an additional 1 cm in length and width along the visible, apparently normal, white matter tracts adjacent to the tumor to create the DTI-PTV. DTI-CTV was smaller when compared to a conventional T2-weighted CTV ($p < 0.005$), thus suggesting that DTI-CTV may detect more specifically tumor invasion rather than tumor plus peritumoral edema, as for T2-weighted CTV. Compared to the conventional PTV, the DTI-PTV showed a trend towards volume reduction. It is worth noting that, although these DTI-based volumes were smaller than conventional volumes, they still included sites of tumor recurrence. As such, the extension of CTV along the abnormal tensor tracts preserves coverage of glioma cells' routes of spreading whilst sparing uninvolved brain, which seems a promising approach to individualize RT planning for GBM patients [62].

In light of these feasibility studies, a multicenter, prospective longitudinal observational cohort study in patients with GBM is ongoing (PRaM-GBM, trial NCT03294434, estimated study completion by June 2021) to establish a DTI-based model that could accurately predict where GBM will progress after treatment, therefore evaluating its utility to optimize radiation treatment planning. In this study, a comparison of amino-acid PET and perfusion-derived rCBV with DTI biomarker is also planned.

More recently, Jordan et al. proposed an innovative approach to combine MR tractography in RT planning by developing a tool for translating a tractography dataset into a white matter path length (WMPL) map. In this map, each voxel's quantitative value represents the minimum distance (in mm) between the voxel and the GTV along white matter pathways [27]. These WMPL maps can be loaded into an RT planning software to modify the treatment volume anisotropically. The method was tested in a retrospective cohort of 13 GBM patients, three of whom had marginal recurrences using a standard isotropic technique. Using WMPL to define target volumes, two of three marginal recurrences would have been included in the target volume, and all other recurrences would have remained within the target volume, with a median target volume 19% smaller than the isotropic technique. This proof-of-concept work lays the groundwork for future studies to evaluate the clinical value of incorporating tractography modeling into treatment planning [27].

The integration of MR tractography has also been proposed in the context of inverse planning, by defining a target dose to the tumor tissue and dose-volume constraints to relevant white matter tracts, and then determining, via an optimization process, the treatment plan which best matches all the input criteria. Wang et al. used DTI and functional MRI cortical activations (BOLD-fMRI) to localize the motor corticospinal tracts (CSTs) and primary motor cortices in a retrospective cohort of 20 patients with HGG [65]. For each patient, three different treatment plans were considered: A three-dimensional conformal radiation treatment (3DCRT) plan and an IMRT plan, both considering the standard morphological organs at risk (OARs), as well an IMRT plan which also included CSTs and primary motor cortices (PMCs) among the OARs. The authors found that the maximum and mean dose (Dmax and Dmean) to the ipsilateral and contralateral PMC and CST regions were considerably decreased in the IMRT plans, including tractography and fMRI data, possibly reducing the probability of late radiation injury to these structures [65]. Similar results of dose-reduction to relevant white matter tracts located near the RT target volumes were described in another study from Igaki et al., which incorporated the CST as OAR in the IMRT plan of GBM and comparing the dose sparing with respect to conventional IMRT [66].

More recently, Altabella et al. evaluated the feasibility of integrating multiple white matter tracts as depicted by MR tractography in the tomotherapy RT planning in a retrospective dosimetric study of 19 HGG patients [67]. The authors evaluated three intra-hemispheric associative fiber bundles involved in language or visuospatial attention networks (superior longitudinal fascicle, inferior fronto-occipital fascicle, and uncinate fascicle) and the projection motor fibers of the CST. For all patients, the original plans without tracts were compared with the optimized plans incorporating the fibers, the latter demonstrating a significant Dmean and Dmax reduction for most of the tracts, with more relevant dose sparing for contralateral tracts ($p < 0.0001$) and without significant differences in terms of PTV [67]. Future studies are warranted to assess the clinical benefits of MR tractography-guided dose sparing on long-term cognitive dysfunctions and the impact of this approach on patients' neurological outcomes and quality of life.

3. PET Radiopharmaceuticals for RT Planning of Gliomas: Physiology and Clinical Results

3.1. Amino Acid Analogs

Amino acid PET tracers, namely, [^{11}C]methyl-l-methionine (MET), O-(2-[^{18}F]fluoroethyl)-l-tyrosine (FET) and 3,4-dihydroxy-6-[^{18}F]fluoro-l-phenylalanine (F-DOPA), are now being successfully used in the management of patients with primary or secondary brain tumors [23][68][69]. In contrast to [^{18}F]Fluorodeoxyglucose (FDG), they are characterized by high tumor-to-background ratios (TBR), making them the radiopharmaceuticals of choice in brain tumor imaging. The cellular

uptake of radiolabeled amino acids is based on the expression of the sodium-independent large neutral amino acid transporters LAT1 and LAT2 on tumor cells [70]. This mechanism is independent of BBB permeability, enabling radiolabeled amino acids to depict non-contrast-enhancing tumor portions, including during anti-angiogenic therapy [71][72][73]. On the other hand, unspecific uptake may occur at sites of BBB disruption and inflammation [74]. Additionally, there are recent reports showing that concomitant therapies with dexamethasone or temozolomide have an impact on amino acid uptake of normal-appearing brain structures [75][76][77]. These variables should be carefully evaluated in light of potential effects on target delineation, particularly in the recurrent setting.

With the exception of MET, amino acid radiopharmaceuticals are not incorporated into proteins. Despite this and other biological differences, including the metabolism of F-DOPA by the aromatic amino acid decarboxylase in dopaminergic and serotoninergic neurons, no significant differences in terms of tumor detection have been shown between the three most widely available radiolabeled amino acids [25][26][27].

Amino acid PET has shown better accuracy than standard MRI in the definition of brain tumor extent [28], and its inclusion in the surgical planning demonstrated a positive impact on survival [29]. Additionally, the biological tumor volume (BTV) identified by amino acid PET demonstrated a significant prognostic value either after surgery [30] or after postoperative chemo/radiotherapy in GBM. These findings provide a strong rationale for the incorporation of amino acid PET in RT planning [31] (Figure 1).

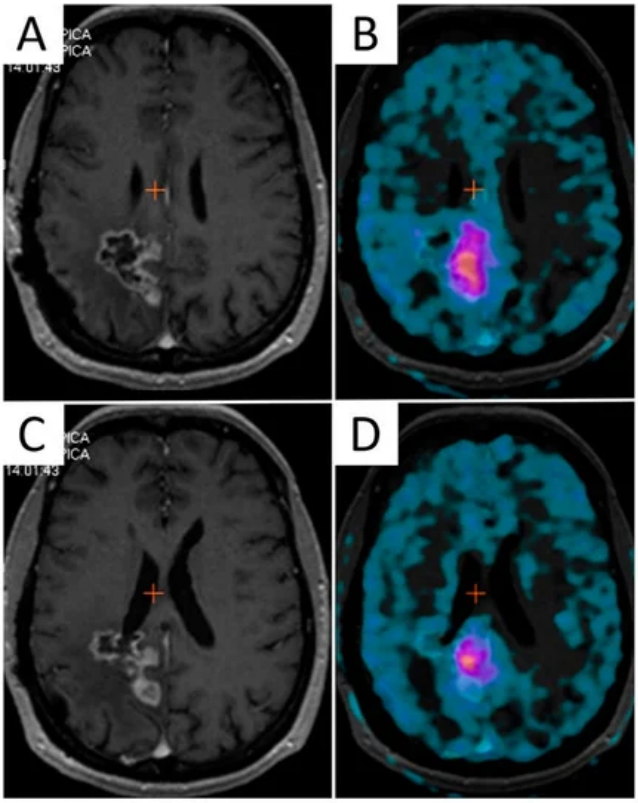

Figure 1. The mismatch between contrast-enhanced T1-weighted MRI and 3,4-dihydroxy-6-[^{18}F]fluoro-L-phenylalanine (F-DOPA) PET/CT in a 45-year-old female patient with recurrent GBM after multimodal first-line therapy. Two axial contrast-enhanced T1-weighted images (**A**,**C**) along with corresponding F-DOPA PET/CT slices (**B**,**D**) identifying different volumes of disease.

3.1.1. MET

MET was first used for brain tumor imaging about three decades ago and has long been considered the standard PET radiopharmaceutical in this setting. Nevertheless, because of the short half-life of Carbon-11 (20 min), MET cannot be commercialized and is available only to centers having an on-site cyclotron. Several original studies have analyzed the role of MET in radiotherapy planning. As early as 2005, Grosu AL et al. showed that the BTV defined by MET-PET was substantially different from that defined using traditional radiological investigations (MRI or CT) in 39 patients with HGG following surgery. MET tumor uptake, defined by a TBR of 1.7, extended non-uniformly beyond Gd enhancement on MRI in 74% of cases and was identified outside the hyperintensity areas on T2-weighted MRI in 50% of patients. Of note, in 28% of patients, amino acid uptake extended >25 mm beyond the MRI abnormalities seen on contrast-enhanced T1-weighted sequences. In contrast, Gd enhancement and T2 hyperintensities extended outside the MET uptake in 69% and 100% of cases, respectively [32].

These findings have significant implications for target volumes delineation and for sparing normal brain tissue from unnecessary radiation. A later study of Matsuo M et al. in 32 patients with newly diagnosed GBM following surgery showed that a margin of at least 20 mm in T2-weighted sequences is necessary to cover MET PET signal with good accuracy [33]. In this paper, a TBR of 1.3 was chosen as the threshold for malignancy based on the results of a former biopsy-controlled study [34].

Navarria et al. investigated the role of integrated MET and MRI for RT planning in 69 patients with HGG following surgical resection [35]. They found that, in all patients, the BTV defined on MET-PET was included within the CTV based on FLAIR sequences. In contrast, the MET-PET signal was outside the CTV based on contrast-enhanced T1-weighted images in 50% of cases. This suggests that the use of MET would not change the target volumes if these are defined based on FLAIR sequences; nevertheless, the integration of MET could significantly modify the CTV in case this is defined on contrast-enhanced T1-weighted sequences. However, the criteria for the definition of tumor extent on MET PET were not specified in this study [35]. Iuchi et al. designed a study to establish the correlation between postoperative MET uptake and relapse patterns in 22 patients affected by GBM. They established dose thresholds needed to control regions with different tumor-to-background indices on MET. A region with MET TBR < 2.12 might be controlled by a total dose of 60 Gy using standard fractionation (2 Gy/fraction), while a region with MET uptake index < 1.41 might be controlled by a standard total dose of 40 Gy. These results suggest that the optimal radiation dose for tumor control could be determined based on MET uptake in individual cases [36]. The pattern of failure after radiochemotherapy was retrospectively correlated with MET PET, not used for RT planning, by Lee et al. in 26 patients with newly diagnosed GBM. MET-BTV was defined by a threshold of 1.5 times the mean cerebellar uptake. The analysis showed that non-central failures are more common in patients with suboptimal coverage of MET BTV [37].

3.1.2 [^{18}F]FET

The results obtained by Grosu et al. with MET [32] were confirmed by Weber and co-workers in 19 patients with HGG imaged by FET. In this study, the BTV identified by FET using 40% of maximum standardized uptake value (SUVmax) as a threshold for tumor definition, extended more than 20 mm beyond Gd-enhanced GTV in 32% of cases. BTV and GTV were substantially discordant in the majority of patients (95%) [38]. A subsequent analysis of the relapse patterns in 10 patients from the same cohort showed a similar recurrent tumor volume outside either the GTV or the BTV [39]. Using a different threshold for tumor volume definition (i.e., TBR > 1.5) in 17 patients with GBM, other authors concluded that FET-based BTV was significantly larger than MRI-based GTV [40]. Rieken et al. showed that MRI-based PTV would not cover the FET-based GTV in 17% of 41 patients at first irradiation or at recurrence, suggesting that amino acid PET should be routinely included in the RT planning [41]. In line with this, a more recent study showed that the CTV (GTV + 20 mm) based on Gd-enhancement would cover about 90% of the FET-based GTV. In this study, it is speculated that patients with GBM would benefit most from integrating FET in RT planning, as they have larger FET-positive volumes of disease compared to grade III gliomas [42]. Potential candidates to undergo FET-aided RT planning might be particularly those patients with GBMs featuring non-contrast-enhancing tumor portions, which eventually turn out to be FET-positive [43].

Harat et al. prospectively evaluated the integration of dual-time point FET PET, acquired prior to primary radiochemotherapy, on the RT treatment planning and prediction of recurrence of 34 patients with GBM. They showed that PET-based GTV extended beyond GTV plus 20 mm margins in 26.5% cases. Furthermore, the recurrence pattern analysis showed that progressions occurred most often in the FET-GTV than in the MRI-GTV (70% vs. 57% of cases) [44]. These results are in accordance with those of Lundemann et al., who analyzed 50 patients with GBM showing that the overlap between treatment volumes and the recurrent tumor is highest for RT planning integrating contrast-enhanced MRI and PET compared to RT planning based on either modality alone [45]. The pattern of recurrence was also analyzed retrospectively by Fleischmann et al. in 36 patients with GBM who underwent FET PET before primary radiochemotherapy. They showed that integrating FET would reduce the GTV expansion from 20 mm to 15 mm compared to RT planning based on contrast-enhanced MRI alone [46]. These latter studies used the same TBR threshold of 1.6 for tumor contouring on PET [41][42][43][44][45][46]. Finally, a dose escalation strategy based on a FET-adapted RT boost has been evaluated prospectively with no apparent clinical benefit [47]. Nevertheless, a follow-up study of GBM relapse patterns after FET-adapted radiotherapy showed that a CTV based on FET + 7 mm margin would cover 100% of relapses, while significantly reducing the PTV [48].

3.1.3 F-DOPA

F-DOPA PET has been more rarely used for RT planning of brain gliomas so far. Kosztyla et al. compared target delineation using MRI and F-DOPA PET in 19 patients with newly diagnosed HGG. They found that PET-based volumes were significantly larger than MRI-based volumes. Nevertheless, all but one documented recurrence extended beyond the PET GTV, and most were contained by a 20 mm margin on the MRI GTV. Therefore, they concluded that it is unclear whether treatment planning using F-DOPA PET would yield better treatment outcomes. A major limitation of this work was

that the criteria for PET positivity were not specified [49]. In a later study, the same authors investigated the feasibility of using F-DOPA PET for dose painting with volumetric modulated arc therapy (VMAT) in 10 patients with HGG. F-DOPA PET could achieve dose-escalated coverage to BTV without increasing the dose to cranial OARs, suggesting that this approach would offer better disease control than conventional RT for HGG [50].

Potential advantages and current limitations of advanced MRI techniques and amino acid PET for first-line RT planning of glioma have been summarized in Table 1

Table 1. Summary of findings on advanced imaging techniques for first-line RT planning of gliomas.

First Line RT Treatment					
Advanced Imaging Modality	**RT Planning Technique**	**Retrospective/ Simulation Studies Available**	**Prospective Studies Available**	**Potential Advantages**	**Limitations**
MRSI	**Dose escalation and GTV expansion based on increased Cho/NAA ratio**	**YES**	**YES**	**Reduced marginal and in-field recurrence, improved survival outcomes, reduced toxicity**	**Technically demanding**
dMRI (ADC)	**Dose escalation and GTV expansion on regions with reduced ADC (hypercellularity)**	**NO**	**NO**	**Better definition of hypercellular subvolumes identified by high b-value dMRI**	**EPI distortions may hamper image registration to define a boost or adaptive target**
DTI	**Anisotropic PTV expansion based on DTI abnormality (peritumoral microinfiltration); Dose painting**	**YES**	**NO**	**Better planning conformation according to tumor infiltrating pattern: Reduced toxicity and reduced out-of-field recurrences**	**Limited data available on survival benefit**
MR Tractography	**Inverse planning using eloquent tracts as OAR**	**YES**	**NO**	**Reduced toxicity, improved quality of life**	**No data on the impact on long-term cognitive dysfunction**
PWI	**Dose escalation and GTV expansion on regions with increased rCBV**	**NO**	**NO**	**Better definition of hypervascular areas; better tumor coverage**	**Lack of standardization of PWI acquisition and analysis; no data available on survival benefit**
Amino acid PET [1]	**Inclusion of PET-BTV in RT planning**	**YES**	**YES**	**Better tumor coverage; better tumor control**	**Modification of RT planning depends on the PET segmentation method; limited data on survival benefit**

[1] Different amino acid radiopharmaceuticals are considered equivalent. NAA, N-acetyl-aspartate; Cho, choline; DTI, diffusion tensor imaging; OAR, organs at risk; PWI, perfusion MRI; BTV, biological tumor volume.

References

1. Le Bihan, D. Looking into the functional architecture of the brain with diffusion MRI. Nat. Rev. Neurosci. 2003, 4, 469–480.
2. Beaulieu, C. The basis of anisotropic water diffusion in the nervous system—A technical review. NMR Biomed. 2002, 15, 435–455.
3. Jones, D.K. Studying connections in the living human brain with diffusion MRI. Cortex 2008, 44, 936–952.
4. Jellison, B.J.; Field, A.S.; Medow, J.; Lazar, M.; Salamat, M.S.; Alexander, A.L. Diffusion tensor imaging of cerebral white matter: A pictorial review of physics, fiber tract anatomy, and tumor imaging patterns. AJNR Am. J. Neuroradiol. 2004, 25, 356–369.
5. Castellano, A.; Cirillo, S.; Bello, L.; Riva, M.; Falini, A. Functional MRI for Surgery of Gliomas. Curr. Treat. Opt. Neurol. 2017, 19, 34.

6. Giese, A.; Bjerkvig, R.; Berens, M.; Westphal, M. Cost of migration: Invasion of malignant gliomas and implications for t reatment. J. Clin. Oncol. 2003, 21, 1624–1636.
7. Giese, A.; Westphal, M. Glioma invasion in the central nervous system. Neurosurgery 1996, 39, 235–252.
8. Jbabdi, S.; Mandonnet, E.; Duffau, H.; Capelle, L.; Swanson, K.R.; Pélégrini-Issac, M.; Guillevin, R.; Benali, H. Simulati on of anisotropic growth of low-grade gliomas using diffusion tensor imaging. Magn. Reson. Med. Off. J. Int. Soc. Mag n. Reson. Med. 2005, 54, 616–624.
9. Sternberg, E.J.; Lipton, M.L.; Burns, J. Utility of diffusion tensor imaging in evaluation of the peritumoral region in patien ts with primary and metastatic brain tumors. AJNR Am. J. Neuroradiol. 2014, 35, 439–444.
10. Price, S.; Jena, R.; Burnet, N.; Hutchinson, P.; Dean, A.; Pena, A.; Pickard, J.; Carpenter, T.; Gillard, J. Improved deline ation of glioma margins and regions of infiltration with the use of diffusion tensor imaging: An image-guided biopsy stud y. Am. J. Neuroradiol. 2006, 27, 1969–1974.
11. Price, S.J.; Jena, R.; Burnet, N.G.; Carpenter, T.A.; Pickard, J.D.; Gillard, J.H. Predicting patterns of glioma recurrence using diffusion tensor imaging. Eur. Radiol. 2007, 17, 1675–1684.
12. Krishnan, A.P.; Asher, I.M.; Davis, D.; Okunieff, P.; O'Dell, W.G. Evidence that MR diffusion tensor imaging (tractograph y) predicts the natural history of regional progression in patients irradiated conformally for primary brain tumors. Int. J. Radiat. Oncol. Biol. Phys. 2008, 71, 1553–1562.
13. Jordan, K.; Morin, O.; Wahl, M.; Amirbekian, B.; Chapman, C.; Owen, J.; Mukherjee, P.; Braunstein, S.; Henry, R. An O pen-Source Tool for Anisotropic Radiation Therapy Planning in Neuro-oncology Using DW-MRI Tractography. Front. On col. 2019, 9, 810.
14. Berberat, J.; McNamara, J.; Remonda, L.; Bodis, S.; Rogers, S. Diffusion tensor imaging for target volume definition in glioblastoma multiforme. Strahlenther. Onkol. 2014, 190, 939–943.
15. Jena, R.; Price, S.; Baker, C.; Jefferies, S.; Pickard, J.; Gillard, J.; Burnet, N. Diffusion tensor imaging: Possible implicat ions for radiotherapy treatment planning of patients with high-grade glioma. Clin. Oncol. 2005, 17, 581–590.
16. Jensen, M.B.; Guldberg, T.L.; Harboll, A.; Lukacova, S.; Kallehauge, J.F. Diffusion tensor magnetic resonance imaging driven growth modeling for radiotherapy target definition in glioblastoma. Acta Oncol. 2017, 56, 1639–1643.
17. Wang, M.; Ma, H.; Wang, X.; Guo, Y.; Xia, X.; Xia, H.; Guo, Y.; Huang, X.; He, H.; Jia, X.; et al. Integration of BOLD-fM RI and DTI into radiation treatment planning for high-grade gliomas located near the primary motor cortexes and cortico spinal tracts. Radiat. Oncol. 2015, 10, 64.
18. Igaki, H.; Sakumi, A.; Mukasa, A.; Saito, K.; Kunimatsu, A.; Masutani, Y.; Hanakita, S.; Ino, K.; Haga, A.; Nakagawa, K. Corticospinal tract-sparing intensity-modulated radiotherapy treatment planning. Rep. Pract. Oncol. Radiother. 2014, 1 9, 310–316.
19. Altabella, L.; Broggi, S.; Mangili, P.; Conte, G.M.; Pieri, V.; Iadanza, A.; Del Vecchio, A.; Anzalone, N.; di Muzio, N.; Cala ndrino, R.; et al. Integration of Diffusion Magnetic Resonance Tractography into tomotherapy radiation treatment planni ng for high-grade gliomas. Phys. Med. 2018, 55, 127–134.
20. Einstein, D.B.; Wessels, B.; Bangert, B.; Fu, P.; Nelson, A.D.; Cohen, M.; Sagar, S.; Lewin, J.; Sloan, A.; Zheng, Y.; et a l. Phase II trial of radiosurgery to magnetic resonance spectroscopy-defined high-risk tumor volumes in patients with gli oblastoma multiforme. Int. J. Radiat. Oncol. Biol. Phys. 2012, 84, 668–674.
21. Laprie, A.; Ken, S.; Filleron, T.; Lubrano, V.; Vieillevigne, L.; Tensaouti, F.; Catalaa, I.; Boetto, S.; Khalifa, J.; Attal, J.; et al. Dose-painting multicenter phase III trial in newly diagnosed glioblastoma: The SPECTRO-GLIO trial comparing arm A standard radiochemotherapy to arm B radiochemotherapy with simultaneous integrated boost guided by MR spectros copic imaging. BMC Cancer 2019, 19, 167.
22. Gurbani, S.; Weinberg, B.; Cooper, L.; Mellon, E.; Schreibmann, E.; Sheriff, S.; Maudsley, A.; Goryawala, M.; Shu, H.K.; Shim, H. The Brain Imaging Collaboration Suite (BrICS): A Cloud Platform for Integrating Whole-Brain Spectroscopic M RI into the Radiation Therapy Planning Workflow. Tomography 2019, 5, 184–191.
23. Andronesi, O.C.; Loebel, F.; Bogner, W.; Marjańska, M.; Vander Heiden, M.G.; Iafrate, A.J.; Dietrich, J.; Batchelor, T.T.; Gerstner, E.R.; Kaelin, W.G. Treatment response assessment in IDH-mutant glioma patients by noninvasive 3D functio nal spectroscopic mapping of 2-hydroxyglutarate. Clin. Cancer Res. 2016, 22, 1632–1641.
24. Choi, C.; Raisanen, J.M.; Ganji, S.K.; Zhang, S.; McNeil, S.S.; An, Z.; Madan, A.; Hatanpaa, K.J.; Vemireddy, V.; Shepp ard, C.A. Prospective longitudinal analysis of 2-hydroxyglutarate magnetic resonance spectroscopy identifies broad clin ical utility for the management of patients with IDH-mutant glioma. J. Clin. Oncol. 2016, 34, 4030.
25. Jafari-Khouzani, K.; Loebel, F.; Bogner, W.; Rapalino, O.; Gonzalez, G.R.; Gerstner, E.; Chi, A.S.; Batchelor, T.T.; Rose n, B.R.; Unkelbach, J.; et al. Volumetric relationship between 2-hydroxyglutarate and FLAIR hyperintensity has potentia l implications for radiotherapy planning of mutant IDH glioma patients. Neuro Oncol. 2016, 18, 1569–1578.

26. Cicone, F.; Carideo, L.; Scaringi, C.; Romano, A.; Mamede, M.; Papa, A.; Tofani, A.; Cascini, G.L.; Bozzao, A.; Scopinaro, F.; et al. Long-term metabolic evolution of brain metastases with suspected radiation necrosis following stereotactic radiosurgery: Longitudinal assessment by F-DOPA PET. Neuro Oncol. 2020.

27. Habermeier, A.; Graf, J.; Sandhöfer, B.F.; Boissel, J.P.; Roesch, F.; Closs, E.I. System L amino acid transporter LAT1 accumulates O-(2-fluoroethyl)-L-tyrosine (FET). Amino Acids 2015, 47, 335–344.

28. Wirsching, H.-G.; Roelcke, U.; Weller, J.; Hundsberger, T.; Hottinger, A.F.; von Moos, R.; Caparrotti, F.; Conen, K.; Remonda, L.; Roth, P. MRI and 18FET-PET Predict Survival Benefit from Bevacizumab Plus Radiotherapy in Patients with Isocitrate Dehydrogenase Wild-type Glioblastoma: Results from the Randomized ARTE Trial. Clin. Cancer Res. 2021, 27, 179–188.

29. Hutterer, M.; Nowosielski, M.; Putzer, D.; Waitz, D.; Tinkhauser, G.; Kostron, H.; Muigg, A.; Virgolini, I.J.; Staffen, W.; Trinka, E. O-(2-18F-fluoroethyl)-L-tyrosine PET predicts failure of antiangiogenic treatment in patients with recurrent high-grade glioma. J. Nucl. Med. 2011, 52, 856–864.

30. Galldiks, N.; Dunkl, V.; Ceccon, G.; Tscherpel, C.; Stoffels, G.; Law, I.; Henriksen, O.M.; Muhic, A.; Poulsen, H.S.; Steger, J. Early treatment response evaluation using FET PET compared to MRI in glioblastoma patients at first progression treated with bevacizumab plus lomustine. Eur. J. Nucl. Med. Mol. Imaging 2018, 45, 2377–2386.

31. Hutterer, M.; Nowosielski, M.; Putzer, D.; Jansen, N.L.; Seiz, M.; Schocke, M.; McCoy, M.; Göbel, G.; La Fougère, C.; Virgolini, I.J. [18F]-fluoro-ethyl-L-tyrosine PET: A valuable diagnostic tool in neuro-oncology, but not all that glitters is glioma. Neuro Oncol. 2013, 15, 341–351.

32. Carideo, L.; Minniti, G.; Mamede, M.; Scaringi, C.; Russo, I.; Scopinaro, F.; Cicone, F. (18)F-DOPA uptake parameters in glioma: Effects of patients' characteristics and prior treatment history. Br. J. Radiol. 2018, 91, 20170847.

33. Stegmayr, C.; Stoffels, G.; Kops, E.R.; Lohmann, P.; Galldiks, N.; Shah, N.J.; Neumaier, B.; Langen, K.J. Influence of Dexamethasone on O-(2-[(18)F]-Fluoroethyl)-L-Tyrosine Uptake in the Human Brain and Quantification of Tumor Uptake. Mol. Imaging Biol. 2019, 21, 168–174.

34. Cicone, F.; Carideo, L.; Minniti, G.; Scopinaro, F. The mean striatal (18)F-DOPA uptake is not a reliable cut-off threshold for biological tumour volume definition of glioma. Eur. J. Nucl. Med. Mol. Imaging 2019, 46, 1051–1053.

35. Becherer, A.; Karanikas, G.; Szabó, M.; Zettinig, G.; Asenbaum, S.; Marosi, C.; Henk, C.; Wunderbaldinger, P.; Czech, T.; Wadsak, W.; et al. Brain tumour imaging with PET: A comparison between [18F]fluorodopa and [11C]methionine. Eur. J. Nucl. Med. Mol. Imaging 2003, 30, 1561–1567.

36. Grosu, A.L.; Astner, S.T.; Riedel, E.; Nieder, C.; Wiedenmann, N.; Heinemann, F.; Schwaiger, M.; Molls, M.; Wester, H.J.; Weber, W.A. An interindividual comparison of O-(2-[18F]fluoroethyl)-L-tyrosine (FET)- and L-[methyl-11C]methionine (MET)-PET in patients with brain gliomas and metastases. Int. J. Radiat. Oncol. Biol. Phys. 2011, 81, 1049–1058.

37. Kratochwil, C.; Combs, S.E.; Leotta, K.; Afshar-Oromieh, A.; Rieken, S.; Debus, J.; Haberkorn, U.; Giesel, F.L. Intra-Individual comparison of ^{18}F-FET and ^{18}F-DOPA in PET imaging of recurrent brain tumors. Neuro Oncol. 2014, 16, 434–440.

38. Pauleit, D.; Floeth, F.; Hamacher, K.; Riemenschneider, M.J.; Reifenberger, G.; Müller, H.W.; Zilles, K.; Coenen, H.H.; Langen, K.J. O-(2-[18F]fluoroethyl)-L-tyrosine PET combined with MRI improves the diagnostic assessment of cerebral gliomas. Brain 2005, 128, 678–687.

39. Pirotte, B.J.; Levivier, M.; Goldman, S.; Massager, N.; Wikler, D.; Dewitte, O.; Bruneau, M.; Rorive, S.; David, P.; Brotchi, J. Positron emission tomography-guided volumetric resection of supratentorial high-grade gliomas: A survival analysis in 66 consecutive patients. Neurosurgery 2009, 64, 471–481.

40. Poulsen, S.H.; Urup, T.; Grunnet, K.; Christensen, I.J.; Larsen, V.A.; Jensen, M.L.; Af Rosenschöld, P.M.; Poulsen, H.S.; Law, I. The prognostic value of FET PET at radiotherapy planning in newly diagnosed glioblastoma. Eur. J. Nucl. Med. Mol. Imaging 2017, 44, 373–381.

41. Piroth, M.D.; Pinkawa, M.; Holy, R.; Klotz, J.; Nussen, S.; Stoffels, G.; Coenen, H.H.; Kaiser, H.J.; Langen, K.J.; Eble, M.J. Prognostic value of early [18F]fluoroethyltyrosine positron emission tomography after radiochemotherapy in glioblastoma multiforme. Int. J. Radiat. Oncol. Biol. Phys. 2011, 80, 176–184.

42. Grosu, A.L.; Weber, W.A.; Riedel, E.; Jeremic, B.; Nieder, C.; Franz, M.; Gumprecht, H.; Jaeger, R.; Schwaiger, M.; Molls, M. L-(methyl-11C) methionine positron emission tomography for target delineation in resected high-grade gliomas before radiotherapy. Int. J. Radiat. Oncol. Biol. Phys. 2005, 63, 64–74.

43. Matsuo, M.; Miwa, K.; Tanaka, O.; Shinoda, J.; Nishibori, H.; Tsuge, Y.; Yano, H.; Iwama, T.; Hayashi, S.; Hoshi, H.; et al. Impact of [11C]methionine positron emission tomography for target definition of glioblastoma multiforme in radiation therapy planning. Int. J. Radiat. Oncol. Biol. Phys. 2012, 82, 83–89.

44. Kracht, L.W.; Miletic, H.; Busch, S.; Jacobs, A.H.; Voges, J.; Hoevels, M.; Klein, J.C.; Herholz, K.; Heiss, W.D. Delineation of brain tumor extent with [11C]L-methionine positron emission tomography: Local comparison with stereotactic histopathology. Clin. Cancer Res. 2004, 10, 7163–7170.
45. Navarria, P.; Reggiori, G.; Pessina, F.; Ascolese, A.M.; Tomatis, S.; Mancosu, P.; Lobefalo, F.; Clerici, E.; Lopci, E.; Bizzi, A.; et al. Investigation on the role of integrated PET/MRI for target volume definition and radiotherapy planning in patients with high grade glioma. Radiother. Oncol. 2014, 112, 425–429.
46. Iuchi, T.; Hatano, K.; Uchino, Y.; Itami, M.; Hasegawa, Y.; Kawasaki, K.; Sakaida, T.; Hara, R. Methionine Uptake and Required Radiation Dose to Control Glioblastoma. Int. J. Radiat. Oncol. Biol. Phys. 2015, 93, 133–140.
47. Lee, I.H.; Piert, M.; Gomez-Hassan, D.; Junck, L.; Rogers, L.; Hayman, J.; Ten Haken, R.K.; Lawrence, T.S.; Cao, Y.; Tsien, C. Association of 11C-methionine PET uptake with site of failure after concurrent temozolomide and radiation for primary glioblastoma multiforme. Int. J. Radiat. Oncol. Biol. Phys. 2009, 73, 479–485.
48. Weber, D.C.; Zilli, T.; Buchegger, F.; Casanova, N.; Haller, G.; Rouzaud, M.; Nouet, P.; Dipasquale, G.; Ratib, O.; Zaidi, H.; et al. [(18)F]Fluoroethyltyrosine- positron emission tomography-guided radiotherapy for high-grade glioma. Radiat. Oncol. 2008, 3, 44.
49. Weber, D.C.; Casanova, N.; Zilli, T.; Buchegger, F.; Rouzaud, M.; Nouet, P.; Vees, H.; Ratib, O.; Dipasquale, G.; Miralbell, R. Recurrence pattern after [(18)F]fluoroethyltyrosine-positron emission tomography-guided radiotherapy for high-grade glioma: A prospective study. Radiother. Oncol. 2009, 93, 586–592.
50. Niyazi, M.; Geisler, J.; Siefert, A.; Schwarz, S.B.; Ganswindt, U.; Garny, S.; Schnell, O.; Suchorska, B.; Kreth, F.W.; Tonn, J.C.; et al. FET-PET for malignant glioma treatment planning. Radiother. Oncol. 2011, 99, 44–48.
51. Rieken, S.; Habermehl, D.; Giesel, F.L.; Hoffmann, C.; Burger, U.; Rief, H.; Welzel, T.; Haberkorn, U.; Debus, J.; Combs, S.E. Analysis of FET-PET imaging for target volume definition in patients with gliomas treated with conformal radiotherapy. Radiother. Oncol. 2013, 109, 487–492.
52. Munck Af Rosenschold, P.; Costa, J.; Engelholm, S.A.; Lundemann, M.J.; Law, I.; Ohlhues, L.; Engelholm, S. Impact of [18F]-fluoro-ethyl-tyrosine PET imaging on target definition for radiation therapy of high-grade glioma. Neuro Oncol. 2015, 17, 757–763.
53. Hayes, A.R.; Jayamanne, D.; Hsiao, E.; Schembri, G.P.; Bailey, D.L.; Roach, P.J.; Khasraw, M.; Newey, A.; Wheeler, H.R.; Back, M. Utilizing 18F-fluoroethyltyrosine (FET) positron emission tomography (PET) to define suspected nonenhancing tumor for radiation therapy planning of glioblastoma. Pract. Radiat. Oncol. 2018, 8, 230–238.
54. Harat, M.; Małkowski, B.; Makarewicz, R. Pre-Irradiation tumour volumes defined by MRI and dual time-point FET-PET for the prediction of glioblastoma multiforme recurrence: A prospective study. Radiother. Oncol. 2016, 120, 241–247.
55. Lundemann, M.; Costa, J.C.; Law, I.; Engelholm, S.A.; Muhic, A.; Poulsen, H.S.; Munck Af Rosenschold, P. Patterns of failure for patients with glioblastoma following O-(2-[(18)F]fluoroethyl)-L-tyrosine PET- and MRI-guided radiotherapy. Radiother. Oncol. 2017, 122, 380–386.
56. Fleischmann, D.F.; Unterrainer, M.; Schön, R.; Corradini, S.; Maihöfer, C.; Bartenstein, P.; Belka, C.; Albert, N.L.; Niyazi, M. Margin reduction in radiotherapy for glioblastoma through (18)F-fluoroethyltyrosine PET?—A recurrence pattern analysis. Radiother. Oncol. 2020, 145, 49–55.
57. Piroth, M.D.; Pinkawa, M.; Holy, R.; Klotz, J.; Schaar, S.; Stoffels, G.; Galldiks, N.; Coenen, H.H.; Kaiser, H.J.; Langen, K.J.; et al. Integrated boost IMRT with FET-PET-adapted local dose escalation in glioblastomas. Results of a prospective phase II study. Strahlenther. Onkol. 2012, 188, 334–339.
58. Piroth, M.D.; Galldiks, N.; Pinkawa, M.; Holy, R.; Stoffels, G.; Ermert, J.; Mottaghy, F.M.; Shah, N.J.; Langen, K.J.; Eble, M.J. Relapse patterns after radiochemotherapy of glioblastoma with FET PET-guided boost irradiation and simulation to optimize radiation target volume. Radiat. Oncol. 2016, 11, 87.
59. Kosztyla, R.; Chan, E.K.; Hsu, F.; Wilson, D.; Ma, R.; Cheung, A.; Zhang, S.; Moiseenko, V.; Benard, F.; Nichol, A. High-Grade glioma radiation therapy target volumes and patterns of failure obtained from magnetic resonance imaging and 18F-FDOPA positron emission tomography delineations from multiple observers. Int. J. Radiat. Oncol. Biol. Phys. 2013, 87, 1100–1106.
60. Kosztyla, R.; Raman, S.; Moiseenko, V.; Reinsberg, S.A.; Toyota, B.; Nichol, A. Dose-Painted volumetric modulated arc therapy of high-grade glioma using 3,4-dihydroxy-6-[(18)F]fluoro-L-phenylalanine positron emission tomography. Br. J. Radiol. 2019, 92, 20180901.